JOURNAL OF PROPULSION AND POWER
Vol. 25, No. 3, May–June 2009

Technical Notes

TECHNICAL NOTES are short manuscripts describing new developments or important results of a preliminary nature. These Notes should not exceed 2500 words (where a figure or table counts as 200 words). Following informal review by the Editors, they may be published within a few months of the date of receipt. Style requirements are the same as for regular contributions (see inside back cover).

Buzz Instability in a Mixed-Compression Air Intake

P. Vivek* and Sanjay Mittal†
Indian Institute of Technology, Kanpur 208 016, India

DOI: 10.2514/1.39751

I. Introduction

THE buzz instability in an air intake was first observed by Oswatitsch [1]. Ferri and Nucci [2], via detailed experiments on an axisymmetric external compression air intake, attributed the occurrence of buzz instability to the velocity discontinuity across the vortex sheet originating at the intersection of the conical shock and strong shock ahead of the intake entrance. The fluctuations began when this vortex sheet approached the inner surface of the cowling. Dailey [3] attributed the origin of the buzz oscillations to a random pressure pulse from the subsonic diffuser. He related the frequency of oscillations to that of an organ pipe with one end closed and the other end open. Fisher et al. [4] conducted experiments on a rectangular external compression intake with a variable ramp. Two kinds of oscillations were found in their tests: "big" and "little" buzz. They had the same frequency of oscillation but different amplitudes. The little buzz was found to be caused by the flow separation below the cowl and is similar to the Ferri type of buzz. The big buzz, on the other hand, was caused by the separation of the boundary layer along the ramp. It is very similar to the Dailey type of buzz. It was also observed that the little and big buzz occur for lower and higher mass flow reduction, respectively. Trapier et al. [5] conducted an experimental as well as a computational study of flow in a rectangular mixed-compression intake for a Mach number range of 1.8–3.0. Both little and big buzz were observed. The little buzz was of the Ferri type They related the oscillations to the acoustic resonance of the shear layer instabilities under the cowl lip. The big buzz was of the Dailey type and occurred due to the separated flow on the ramp in a supersonic diffuser that blocks the intake. The oscillations were caused due to the periodic filling and discharging of the intake. The oscillation frequency of the little buzz was found to be higher than that of the big buzz.

Efforts to numerically investigate the mixed-compression inlets have been very few. Knight [6,7] studied two- and three-dimensional supersonic diffuser flows in simple geometries using the Reynolds-averaged Navier–Stokes equations. Chan and Liang [8] carried out a numerical study of a two-dimensional mixed-compression inlet whose geometry was similar to the one experimentally studied by Anderson and Wong [9]. Jain and Mittal [10] carried out a finite element flow analysis in a mixed-compression inlet by solving the Euler equations. The starting as well as the unstarting of the intake was studied. Recently, Trapier et al. [11] carried out a detached-eddy simulation and compared the results with their own experiments.

The present work is a part of our ongoing work [10] to study flow in mixed-compression intakes. The viscous effects have been included in this work. The geometry of the inlet is very similar to the one experimentally studied by Anderson and Wong [9]. The governing equations for the flow analysis are the compressible Navier–Stokes equations in the conservation law form. A stabilized finite element formulation based on conservation variables is used to solve the flow equations. The streamline-upwind/Petrov–Galerkin stabilization method [12,13] is employed to stabilize the computations against spurious numerical oscillations due to advection-dominated flows. A shock capturing term is added to the formulation to provide stability to the computations in the presence of discontinuities and large gradients in the flow [14–16]. The time integration of the flow equations is done via the generalized trapezoidal rule. For unsteady computations, we employ a second-order accurate-in-time procedure. The role of bleed in starting/unstarting the intake and controlling the buzz instability is investigated. The flow during the buzz is studied in detail to bring out the difference between the little and big buzz.

II. Problem Setup

The mixed-compression intake that is modeled in this work has two ramps. The first ramp is at an angle of 7 deg to the freestream and its length is 28 in. These numbers for the second ramp are 14 deg and 24.1 in., respectively. The two ramps are followed by a throat and a subsonic diffuser. The total length of the intake is 119.02 in. The specification of backpressure at the exit of the intake leads to flow reversal and, therefore, difficulties in carrying out the numerical computations. To alleviate this difficulty, a duct is attached at the exit of the intake and the backpressure is specified at the end of this duct. The duct walls are assumed to be inviscid so that the duct is associated with minimal pressure loss. The length of the duct is twice that of the intake. The cross-sectional area of the duct, compared with that of the throat, is large enough to allow the startup shock to pass through. Computations with Euler equations for the $M = 3$ were reported in an earlier work [10]. With the viscous flow, the intake is unable to start even without the application of any backpressure. An increase in throat area is used to start the flow. The throat area of the original geometry from Anderson and Wong [9] is referred to as A_{to}.

All the results in this paper are shown with respect to the nondimensionalized variables. The length of the intake is used as the characteristic length to nondimensionalize all the length scales. The origin of the coordinate axis is fixed at the leading edge of the first ramp. The inflow and upper boundaries are located 0.2 and 1.0 units, respectively, from the leading edge of the inlet. The flow internal as well as external to the intake is computed. The vertical location of the upper boundary is chosen such that the shock from the engine cowl leaves the computational domain through the outflow boundary. At the inflow boundary, freestream conditions corresponding to $M = 3$ flow are specified. The density, velocity, and temperature are assigned freestream values. A no-slip condition for the velocity and an adiabatic condition for the heat flux are specified on the walls of the intake. On the upper and lower boundaries of the computational domain, the component of velocity normal to the boundaries is specified to be zero. In addition, the component of the

Received 14 July 2008; revision received 25 December 2008; accepted for publication 26 January 2009.

*Graduate Student, Department of Aerospace Engineering.
†Professor, Department of Aerospace Engineering; smittal@iitk.ac.in.

viscous stress vector along these boundaries and the heat flux vector normal to the boundaries are prescribed zero values. At the outflow boundary, the viscous stress vector is assigned a zero value. The backpressure, p_b, is specified at the exit of the duct except when the outflow is supersonic. Computations are carried out for various values of p_b/p_i, where p_i is the freestream static pressure. They are initiated with freestream conditions in the entire domain.

The bleed at the ramp and cowl is used to control the boundary-layer separation and, therefore, to overcome the startup problem of the intake. The various regions of bleed are shown in Fig. 1. Different combinations of mass flow bled from these regions have been tested. The various cases are listed in Table 1 and are helpful in understanding the effect of the strength of bleed and its spatial extent on the control of flow.

To provide adequate resolution of the boundary layer, a fine structured mesh is generated close to the walls of the intake. In the remaining part of the computational domain, an unstructured mesh is generated via Delaunay triangulation. The mesh consists of 99,777 nodes and 196,926 elements. The adequacy of the mesh is confirmed via a computation on a finer mesh with 157,651 nodes and 311,807 elements. Both meshes results in virtually the same solution for the $M = 3$ and $Re = 10^6$ flow through the air intake for supersonic outflow conditions.

A. Effect of Bleed

In general, larger bleed leads to a more stable boundary layer, and the intake can sustain larger backpressure. Results of the various cases that have been studied are shown in Fig. 2. It is seen from the figure that the bleed downstream of the throat plays a vital role in the performance of the intake. For each bleed distribution and throat geometry, computations are carried out for various values of backpressure. At a certain critical value of p_b/p_i, the shock moves to the throat location. A further increase in backpressure can lead to one of two situations. In the first, the intake can unstart, that is, the normal shock is expelled out of the intake, leading to flow spillage. In the second, the subcritical operation of the intake can lead to buzz. Two kinds of buzz are observed: little and biz buzz [4]. The little buzz [2] is associated with relatively low-pressure amplitude oscillations and typically arises out of shear layer instabilities of the separated boundary layer or slip streams as a result of shock interactions. It occurs in low subcritical conditions. The big buzz [3] refers to larger amplitude oscillations and arises due to the shock-induced boundary-layer separation on the compression ramps. It usually occurs in high subcritical conditions.

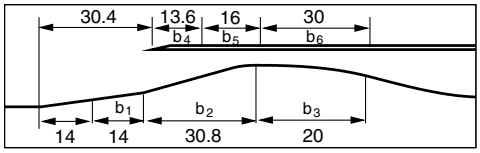

Fig. 1 Boundary-layer bleed configuration. The various regions of bleed are b_1–b_6.

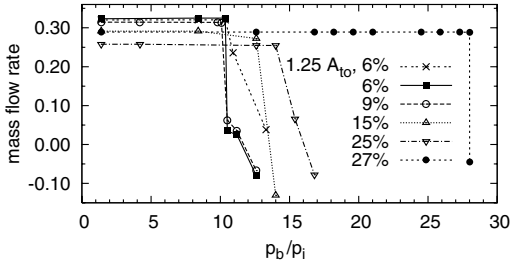

Fig. 2 Variation of the time-averaged mass flow rate at the throat section with backpressure for various bleed configurations; $M_\infty = 3$, $Re = 10^6$ flow in air intake. Unless specified, the throat area is $A_t = 1.14A_{\text{to}}$.

Table 1 Flow in an air intake: various combinations of the bleed that are tested in the computations. $\dot{m}_{b_{\text{total}}}$ is the percentage of the total capture mass flow of the air bled from the intake walls. Its breakup along the six bleed regions shown in Fig. 1 is listed as $\dot{m}_{b_1}$–$\dot{m}_{b_6}$

Case	$\dot{m}_{b_{\text{total}}}$	$\dot{m}_{b_1}$	$\dot{m}_{b_2}$	$\dot{m}_{b_3}$	$\dot{m}_{b_4}$	$\dot{m}_{b_5}$	$\dot{m}_{b_6}$
1	6	——	3.00	——	——	3.00	——
2	9	1.63	3.78	——	1.63	1.91	——
3	15	2.72	6.32	——	2.72	3.19	——
4	25	4.53	10.51	——	4.53	5.31	——
5	27	2.72	6.32	6.05	2.72	3.19	6.00

With $A_t = 1.14A_{\text{to}}$, it is found that 6% bleed is not enough to suppress the massive flow separation at the compression ramps. In fact, in this case, there is no bleed on the first ramp and the cowl tip. Big buzz is observed for the 6% bleed when $10.4 \le p_b/p_i < 12.6$. The intake unstarts for $p_b/p_i = 12.6$. When the bleed is increased to 9%, the flow separation at the cowl tip and first ramp is suppressed to some extent. Therefore, the big buzz does not occur right away. The first ramp and the cowl tip also lie in the regions with boundary-layer bleed for this case. However, the bleed in region b_5 is lower for this case compared with that in the 6% bleed case. Compared with the 6% bleed case, this leads to a stronger shear layer below the cowl near the throat. The appearance of little buzz is observed for $p_b/p_i = 10.5$. Interestingly, after undergoing four to five cycles of little buzz, the flow over the first ramp suffers increased separation, leading to big buzz. Big buzz continues to occur for $p_b/p_i = 11.2$, followed by the unstarting of the intake for larger backpressure. An increase in bleed to 15% causes a disappearance of the big buzz. The flow separation is milder and leads to little buzz for $p_b/p_i = 12.6$. Beyond this backpressure, the normal shock is expelled out of the intake without exhibiting any buzz oscillations. When the bleed is increased to 27% and the bleed region includes all six regions on the ramp and cowl, as shown in Fig. 1 and Table 1, buzz oscillations are not seen for any of the values of backpressure. The normal shock moves back and forth downstream of the throat causing unsteadiness in the flow in that region. However, the oscillations are small and the time-averaged mass flow rate delivered by the intake is quite large.

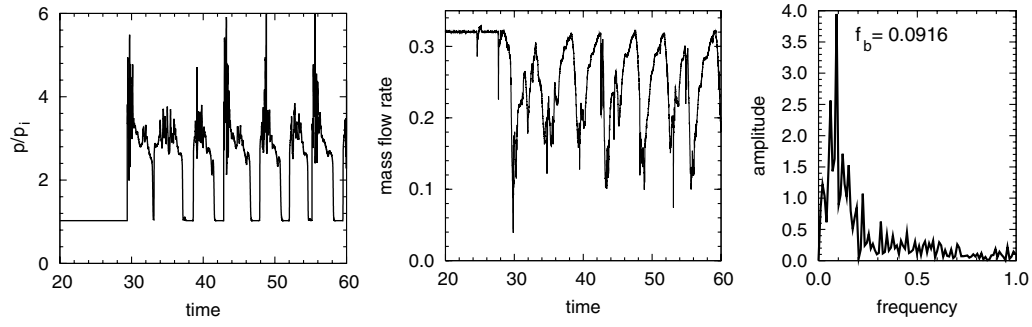

Fig. 3 Time histories of the pressure at a point located at (0.2, 0.1), the mass flow rate at the throat, and the corresponding frequency spectrum; $M_\infty = 3$, $Re = 10^6$, $A_t/A_{\text{to}} = 1.25$, and $p_b/p_i = 10.92$ flow in the air intake with 6% bleed.

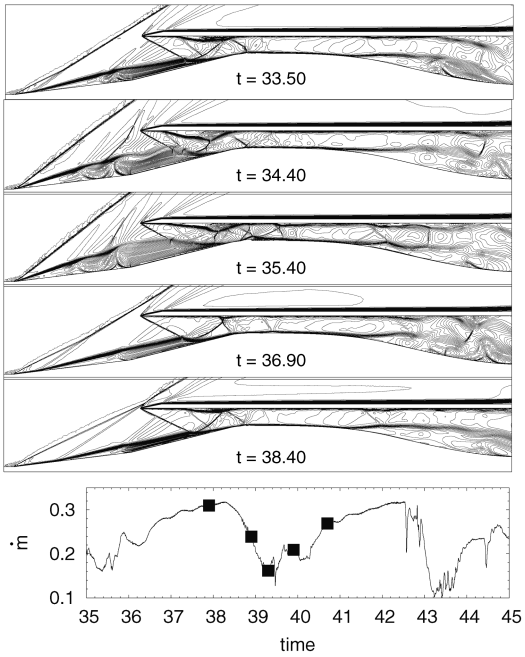

Fig. 4 Mach number distribution at various time instants during one little buzz cycle; ; $M_\infty = 3$, $Re = 10^6$, $A_t/A_{\text{to}} = 1.25$, and $p_b/p_i = 10.92$ flow in the air intake with 6% bleed. Also shown in the bottom row are the time histories of the mass flow rate at the throat.

Beyond $p_b/p_i = 28.0$, the intake unstarts. The effect of an increase of throat area is studied by comparing the case of 6% bleed for $A_t/A_{\text{to}} = 1.14$ and 1.25. Compared with the big buzz observed for $A_t/A_{\text{to}} = 1.14$, $A_t/A_{\text{to}} = 1.25$ experiences little buzz. The intake unstarts for a slightly larger backpressure with the increased throat area.

B. Little Buzz

Figure 3 shows the time histories of the pressure at a point located at (0.2, 0.1) and the mass flow rate at the throat section for the intake with $A_t/A_{\text{to}} = 1.25$, $p_b/p_i = 10.92$, and 6% bleed. A fairly periodic variation is observed. Also shown in the same figure is the frequency spectrum of the time variation of the mass flow rate. These oscillations are very typical of the little buzz instability observed in several earlier studies. The frequency of oscillations is compared with the fundamental acoustic frequency of the air intake. We assume that the entire air intake along with the duct appended at the intake exit behaves as an organ pipe with one end open and the other closed. The downstream end is modeled to be the closed one because of the specification of backpressure, which, therefore, would cause the pressure disturbances to be reflected back. The fundamental acoustic mode is computed using the expression given by Newsome [17]. The nondimensional frequency, based on the freestream speed and length of the intake, is found to be $f_{\text{basic}} = 0.0266$. The nth superharmonic of the mode for a duct with open and closed ends is given by $(2n-1)f_{\text{basic}}$. For the present case, the buzz frequency appears to resonate with the second acoustic mode of the open–closed duct.

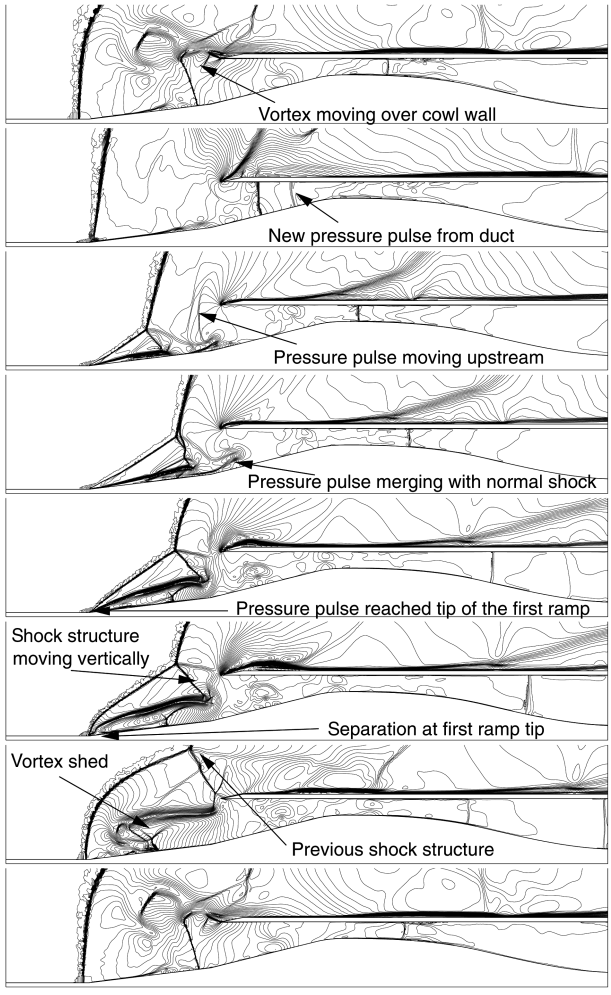

Fig. 6 Mach number distribution at various time instants during one big buzz cycle; $M_\infty = 3$, $Re = 10^6$, $A_t/A_{\text{to}} = 1.14$, $p_b/p_i = 11.2$ flow in the air intake with 9% bleed. Also shown in the bottom row are the time histories of the pressure at a point located at (0.2, 0.1) and the mass flow rate at the throat.

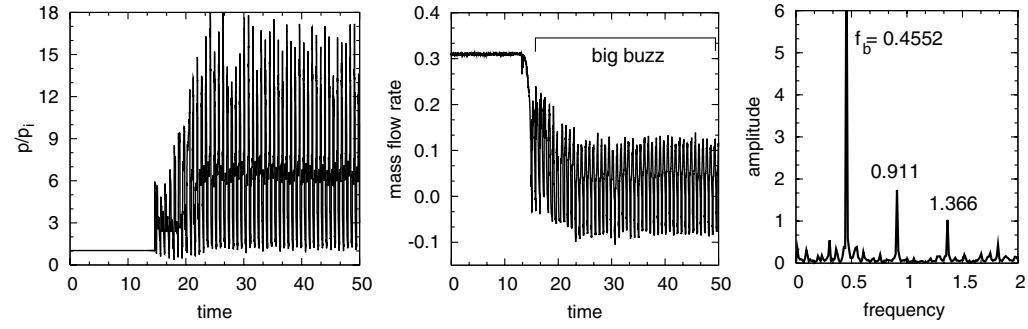

Fig. 5 Time histories of the pressure at a point located at (0.2, 0.1), the mass flow rate at the throat, and the corresponding frequency spectrum for $p_b/p_i = 11.2$; $M_\infty = 3$, $Re = 10^6$, and $A_t/A_{\text{to}} = 1.14$ flow in the air intake with 9% bleed.

The Mach number field at various time instants during one little buzz oscillation is shown in Fig. 4. The first row of the figure corresponds to, approximately, the maximum mass flow rate through the throat. It is also associated with the lowest pressure at the inlet of the intake in the buzz cycle. The separated shear layer becomes unstable downstream of the throat. The oscillation cycle includes the expulsion of shock from the throat region, the increase in the shock angle of the first ramp, and the return of shock back to the throat region. The cyclic nature of the flow separation at the cowl lip can also be seen in the figure.

C. Big Buzz

Figure 5 shows the time histories of the pressure at a point, the mass flow rate at the throat, and the corresponding frequency spectrum for the flow in an intake with $A_t/A_{\text{to}} = 1.14$, $p_b/p_i = 11.2$, and 9% bleed. Big buzz is observed in this case. Compared with the little buzz, the big buzz has higher temporal frequency and larger amplitude oscillations. It also exhibits flow reversal for a significant part of the cycle. Interestingly, as predicted by Dailey [3] for the intake with a longer duct, the big buzz frequency is eighth/ninth organ pipe mode. The frequency as well as the amplitude of the buzz cycles increases with an increase in backpressure.

Figure 6 shows the Mach number field for the unsteady flow at several time instants in one cycle of big buzz for $A_t/A_{\text{to}} = 1.14$, $p_b/p_i = 11.2$, and 9% bleed. The boundary layers on the walls of the subsonic diffuser undergo flow separation due to the normal shock. For $p_b/p_i > 10.5$, the normal shock is pushed upstream of the throat causing the intake to become subcritical. The shock in the convergent part of the intake is unstable and moves upstream, causing the boundary layer on the cowl and ramp surfaces to separate. The separated regions block the flow in the intake. A bow shock forms upstream of the first ramp, as seen in the top row of Fig. 6.

III. Conclusions

The flow in a mixed-compression supersonic intake has been studied via a stabilized finite element method in two dimensions. The effectiveness of bleed in controlling the boundary-layer separation is investigated. Computations are carried out for various values of backpressure. The normal shock moves upstream toward the throat as the backpressure is increased. At the critical condition, it is located at the throat of the intake, at least in a time-averaged sense. As the backpressure is increased further, the intake is pushed in a subcritical state and one of two situations can occur. In the first, the normal shock is completely expelled out of the intake, leading to spillage of flow over the cowl and the unstarting of intake. In the second, buzz is observed. The buzz corresponds to the oscillation of the normal shock as well as the flow in the convergent part of the intake. It is also associated with the cyclic filling and unfilling of the intake. Two kinds of buzz are observed: little and big buzz. The little buzz is found to be a second harmonic, whereas the big buzz is found to be either the eighth or ninth harmonic of the organ pipe mode of the intake duct. It is found that the boundary-layer bleed can be used to control the buzz of an intake. Little buzz is observed for relatively lower bleed. At higher bleed, big buzz is observed. Buzz is completely eliminated when high bleed is implemented, both upstream and downstream of the throat.

Acknowledgment

The partial support for this work by the Aeronautics Research and Development Board, India, is gratefully acknowledged.

References

[1] Oswatitsch, K., "Pressure Recovery for Missiles with Reaction Propulsion at High Supersonic Speeds," NACA TM-1140, 1947.

[2] Ferri, A., and Nucci, R. M., "The Origin of Aerodynamic Instability of Supersonic Inlets at Subcritical Conditions," NACA RM-L50K30, 1951.

[3] Dailey, C. L., "Supersonic Diffuser Instability," *Journal of the Aeronautical Sciences*, Vol. 22, 1955, pp. 733–749.

[4] Fisher, S. A., Neale, M. C., and Brooks, A. J., "On the Sub-Critical Stability of Variable Ramp Intakes at Mach Numbers Around 2," National Gas Turbine Establishment, ARC/R&M-3711, Feb. 1970.

[5] Trapier, S., Duveau, P., and Deck, S., "Experimental Study of Supersonic Inlet Buzz," *AIAA Journal*, Vol. 44, No. 10, 2006, pp. 2354–2365. doi:10.2514/1.20451

[6] Knight, D. D., "Improved Calculation of High Speed Inlet Flows Part II: Results," *AIAA Journal*, Vol. 19, 1981, pp. 172–179. doi:10.2514/3.50939

[7] Knight, D. D., "A Hybrid Explicit-Implicit Numerical Algorithm for the Three-Dimensional Compressible Navier–Stokes Equations" *AIAA Journal*, Vol. 22, 1984, pp. 1056–1063. doi:10.2514/3.8738

[8] Chan, J. J., and Liang, S. M., "Numerical Investigation of Supersonic Mixed-Compression Inlet Using an Upwind Implicit Scheme," *Journal of Propulsion and Power*, Vol. 8, 1992, pp. 158–167. doi:10.2514/3.23456

[9] Anderson, W. E., and Wong, N. D., "Experimental Investigation Of A Large-Scale, Two-Dimensional, Mixed-Compression Inlet System—Performance at Design Conditions, $M_\infty = 3.0$," NASA Ames Research Center TM X-2016, 1970.

[10] Jain, M. K., and Mittal, S., "Euler Flow in a Supersonic Mixed-Compression Inlet," *International Journal for Numerical Methods in Fluids*, Vol. 50, 2006, pp. 1405–1423. doi:10.1002/fld.1109

[11] Trapier, S., Deck, S., and Duveau, P., "Delayed Detached-Eddy Simulation and Analysis of Supersonic Inlet Buzz," *AIAA Journal*, Vol. 46, No. 1, 2008, pp. 118–131. doi:10.2514/1.32187

[12] Hughes, T. J. R., and Brooks, A. N., "A Multi-Dimensional Upwind Scheme with No Crosswind Diffusion," *Finite Element Methods for Convection Dominated Flows*, edited by T. J. R. Hughes, Vol. 34, Applied Mechanics Division, American Society of Mechanical Engineers, New York, 1979, pp. 19–35.

[13] Tezduyar, T. E., and Hughes, T. J. R., "Finite Element Formulations for Convection Dominated Flows with Particular Emphasis on the Compressible Euler Equations," AIAA Paper 83-0125, 1983.

[14] Le Beau, G. J., and Tezduyar, T. E., "Finite Element Computation of Compressible Flows with the SUPG Formulation," *Advances in Finite Element Analysis in Fluid Dynamics*, edited by M. N. Dhaubhadel, M. S. Engelman, and J. N. Reddy, Vol. 123, New York, Fluids Engineering Division, American Society of Mechanical Engineers, New York, 1991, pp. 21–27.

[15] Mittal, S., "Finite Element Computation of Unsteady Viscous Compressible Flows," *Computer Methods in Applied Mechanics and Engineering*, Vol. 157, 1998, pp. 151–175. doi:10.1016/S0045-7825(97)00225-9

[16] Mittal, S., "Finite Element Computation of Unsteady Viscous Compressible Flows Past Stationary Airfoils," *Computational Mechanics*, Vol. 21, 1998, pp. 172–188. doi:10.1007/s004660050293

[17] Newsome, R. W., "Numerical Simulation of Near-Critical and Unsteady, Subcritical Inlet Flow," *AIAA Journal*, Vol. 22, 1984, pp. 1375–1379. doi:10.2514/3.48577

K. Frendi
Associate Editor